Control Engineering Practice 77 (2018) 41–51

Contents lists available at ScienceDirect

Control Engineering Practice

journal homepage: www.elsevier.com/locate/conengprac

A multirate fractional-order repetitive control for laser-based additive manufacturing

D. Wang, X. Chen *

Department of Mechanical Engineering, University of Connecticut, Storrs, CT, 06269, USA

ARTICLE INFO

Keywords:
Selective laser sintering
Laser scanning mechanism
Numerical simulation
Multirate sampled-data control

ABSTRACT

This paper discusses fractional-order repetitive control (RC) to advance the quality of periodic energy deposition in laser-based additive manufacturing (AM). It addresses an intrinsic RC limitation when the exogenous signal frequency cannot divide the sampling frequency of the sensor, e.g., in imaging-based control of fast laser-material interaction in AM. Three RC designs are proposed to address such fractional-order repetitive processes. In particular, a new multirate RC provides superior performance gains by generating high-gain control exactly at the fundamental and harmonic frequencies of exogenous signals. Experimentation on a galvo laser scanner in AM validates effectiveness of the designs.

1. Introduction

Repetitive control (RC) (Inoue, Nakano, Kubo, Matsumoto, & Baba, 1981) is designed to track/reject periodic exogenous signals in applications with repetitive tasks. By learning from memories of previous iterations in the repetitive task, RC can drastically enhance current control performance in the structured task space. Application examples include tracking controls in magnetic and optical disk drives (Chew & Tomizuka, 1989; Doh, Ryoo, & Chung, 2006), wafer scanners (Chen & Tomizuka, 2014), and robotic manipulators (Cosner, Anwar, & Tomizuka, 1990; Meng, Xie, Liu, Lu, & Ai, 2017), as well as regulation controls in wind turbines (Castro, Salton, Flores, Kinnaert, & Coutinho, 2017; Navalkar et al., 2014), power converters (Nazir, Zhou, Watson, & Wood, 2015), and unmanned aerial vehicles (He, Guo, & Leang, 2017).

This paper studies RC in laser-based additive manufacturing (AM) processes, with a focus on the selective laser sintering (SLS) subcategory. This AM technology applies laser beams as the energy source to melt and join powder materials (Schmidt et al., 2017). A typical workpiece is built from many thousands of thin layers. Within each layer, the laser beam is reflected by mirrors driven by periodic or near-periodic reference signals in a beam deflection mechanism (e.g., a dual-axis galvo scanner) to follow trajectories predefined by the part geometry (in a "slicing" process). This process (see, e.g., Fig. 1) contains highly repetitive thermomechanical interactions (Carter, Martin, Withers, & Attallah, 2014; Kruth et al., 2004; Simchi & Pohl, 2003). As a result, periodic errors are introduced in the laser-material interaction and path planning. Indeed, such periodicity has been validated and leveraged upon to improve control processes in other laser-based AM technologies (Heralić, Christiansson, & Lennartson, 2012; Hoelzle & Barton, 2016; Lim, Hoelzle, & Barton, 2017).

To fully release the capability of RC to fundamentally improve the repetitive laser scanning in SLS AM, the internal model principle (Francis & Wonham, 1975; Hara, Yamamoto, Omata, & Nakano, 1988) must be carefully configured in the control design. In digital RC, an internal model $1/(1-z^{-N})$ is implemented in the controller, where z is the complex indeterminate in the z-transform and N is the period of the disturbance/reference. N equals the sampling frequency (denoted in this paper as $1/T_s$ or f_s) divided by the fundamental frequency (f_0) of the periodic signal. When N is an integer, the repetitive controller can generate high gains at the fundamental frequency and its harmonics, yielding small gains in the error-rejection dynamics to create the desired servo performances. When f_s is not divisible by f_0, that is, N is not an integer, RC with the rounded N cannot target the aimed harmonic frequencies exactly, resulting in degraded performances.

Several strategies exist to potentially address problems related to fractional-order periods in RC. Steinbuch, Weiland, and Singh (2007) and Ramos and Costa-Castelló (2012) introduce high-order repetitive controllers with delay elements to widen the high-gain regions around the harmonic frequencies. Nakano, She, Mastuo, and Hino (1996), Yao, Tsai, and Yamamoto (2013), and Chen, Yamada, Sakanushi, and Zhao (2013) employ spatial repetitive controllers in a spatial domain to obtain time-invariant disturbance periods. Cao and Ledwich (2002) and Kurniawan, Cao, and Man (2011) propose adaptive RC schemes where

* Corresponding author.
E-mail addresses: dan.wang@uconn.edu (D. Wang), xchen@uconn.edu (X. Chen).

https://doi.org/10.1016/j.conengprac.2018.05.001
Received 31 January 2018; Received in revised form 11 April 2018; Accepted 9 May 2018

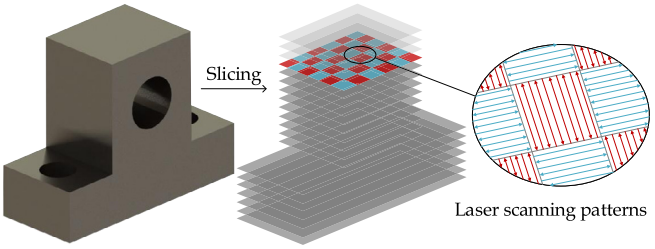

Fig. 1. Schematic of laser scanning patterns in SLS. The example shows the most common "island" pattern in SLS of metallic objects.

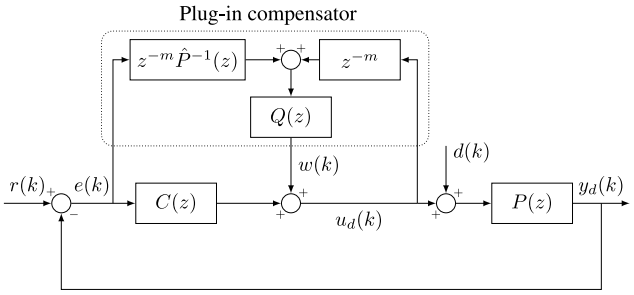

Fig. 2. Block diagram of a plug-in RC design.

the sampling rate is adjusted adaptively to get an integer N. Merry, Kessels, Heemels, Van De Molengraft, and Steinbuch (2011) proposes a delay-varying repetitive controller that uses knowledge of the repetitive variable to continuously adjust the time-varying delay. Nazir et al. (2015), Liu, Zhang, and Zhou (2017), and Zou, Zhou, Wang, and Cheng (2015) design different filters to approximate the fractional orders of delays. Liu, Wang, and Zhou (2016) uses a correction factor to correct the deviated poles of the fractional-order repetitive controller.

Despite the existing literature, it remains not well understood how to create RC *exactly* at the harmonic frequencies in the presence of fractional-order periods and how to systematically analyze the closed-loop performances. To bridge these knowledge gaps, this paper aims at generating enhanced control efforts exactly at desired frequencies in the fractional-order RC. The main result is the development of a multirate RC algorithm and two indirect RC schemes. First, a wide-band RC is achieved by applying the nearest integer of N while widening the attenuation width of each frequency notch in the error-rejection dynamics. In the second indirect RC, a fictitious fundamental frequency is introduced to get an integer N, which creates an overdetermined rejection of the original repetitive errors. The proposed new multirate RC designs the internal model under a second divisible fast sampling frequency f_s' such that $N = f_s'/f_0$ is an integer, and embeds a new zero-phase low-pass filter design to address multirate closed-loop robustness.

Along the course of formulating the multirate RC, an unexpected selective loop-shape modulation is discovered in the intrinsic multirate digital control design. This fundamental behavior, prone to be neglected in the design phase, inspires in the first instance a closed-loop analysis method that exhibits the complete disturbance-attenuation properties of the multirate RC. This analysis method also enables a new design space for applying RC to general systems with mismatched sampling and task periodicity. The remainder of this paper will discuss the theoretical benefits, implementation guidance, and performance comparison of the proposed algorithms. Theoretical analyses are verified by a case study on a galvo scanner in SLS.

A preliminary version of the findings was accepted by the 2018 American Control Conference (Wang & Chen, 2018). This paper substantially extends the research with new theoretical results and illustrative examples. The remainder of this paper is structured as follows. Section 2 reviews a RC design. Two examples in Section 3 elucidate the existence of fractional-order disturbances in SLS. Section 4 builds the proposed fractional-order RC algorithms. Section 5 provides the numerical and experimental verifications of the algorithms. Section 6 concludes the paper.

2. Preliminaries of repetitive control

The proposed fractional-order RC algorithms are based on a plug-in RC design in Fig. 2 (Chen & Tomizuka, 2014). Consider a baseline feedback system composed of the plant $P(z)$ and the baseline controller $C(z)$ (Fig. 2 without the dotted box). $C(z)$ can be designed by means of common servo algorithms, such as PID, H_∞, and lead–lag compensation. The signals $r(k)$, $e(k)$, $d(k)$, and $y_d(k)$ represent, respectively, the reference, the tracking error, the input disturbance, and the system output. Throughout the paper, it is assumed that (1) the coefficients of all transfer functions are real; (2) both $P(z)$ and $C(z)$ are rational, proper, linear, and time-invariant; (3) the baseline feedback loop consisting of $P(z)$ and $C(z)$ is stable.

The plug-in compensator utilizes the internal signals $e(k)$ and $u_d(k)$ to generate a compensation signal $w(k)$. Let m denote the relative degree of $P(z)$, whose nominal model is $\hat{P}(z)$. With the plug-in compensator, the transfer function of the overall controller from $e(k)$ to $u_d(k)$ is

$$C_{all}(z) = \frac{C(z) + z^{-m}\hat{P}^{-1}(z)Q(z)}{1 - z^{-m}Q(z)}. \tag{1}$$

If $Q = (1-\alpha^N)z^{m-N}/(1-\alpha^N z^{-N})$, that is,

$$1 - z^{-m}Q(z) = \frac{1 - z^{-N}}{1 - \alpha^N z^{-N}}, \tag{2}$$

where $\alpha \in [0, 1)$ is a tuning factor that determines the attenuation bandwidth of $1 - z^{-m}Q(z)$, then at the harmonic frequencies ($\omega_k = k2\pi f_0 T_s$, $k \in \mathbb{Z}^+$, the set of positive integers), the magnitude responses of $1 - z^{-m}Q(z)$ are zero because $1 - \mathrm{e}^{-j\omega_k N} = 1 - \mathrm{e}^{-jk2\pi f_0 T_s/(f_0 T_s)} = 1 - \mathrm{e}^{-jk2\pi} = 0$. Hence, $|C_{all}(z)| \to \infty$ and $G_{d\to y_d}(z) = \frac{P(z)[1-z^{-m}Q(z)]}{1+P(z)C(z)} = 0$ when $z = \mathrm{e}^{j\omega_k}$. At the intermediate frequencies, $Q(\mathrm{e}^{j\omega}) \approx 0$, and $|1 - z^{-m}Q(z)|_{z=\mathrm{e}^{j\omega}} \approx 1$ when α is close to 1; thus $C_{all}(z) \approx C(z)$, and the original loop shape is maintained. Choosing a smaller α can yield a wider attenuation bandwidth, at the cost of deviating from the baseline loop shape.

Note that for $Q(z)$ in (2) to be implementable, the disturbance period N should be greater than the relative degree m, which is commonly satisfied in sampled-data regulation control. For instance, in the multirate RC example in Section 5, $N = 40 > m = 3$. Indeed, since the closed-loop bandwidth (B_p) is designed to cover the fundamental disturbance frequency f_0 and B_p is no less than 10% of the Nyquist frequency ($f_s/2$) from principles of feedback design, common control practice thus renders $N = f_s/f_0$ to be greater than 20. That is, N is at least one order of magnitude larger than the relative degree of the plant model under principles of feedback design.

During implementation, zero-phase pairs $q_j(z^{-1})q_j(z)$ ($j \in \mathbb{Z}$) are additionally incorporated into $Q(z)$ for robustness against plant uncertainties at high-frequency regions:

$$Q(z) = \frac{(1-\alpha^N)z^{-(N-m)}}{1-\alpha^N z^{-N}} \prod_{j=0}^{M} q_j(z^{-1})q_j(z), \tag{3}$$

where $M \in \mathbb{Z}$ is determined according to the design requirements. For instance, the following design of $q_i(z)$ ($i \in \mathbb{Z}^+$) places four zeros of $Q(z)$ at $\mathrm{e}^{\pm j\Omega_i T_s'}$ to make its frequency response equal zero at Ω_i:

$$q_i(z) = \frac{1 - 2\cos(\Omega_i T_s)z + z^2}{2 - 2\cos(\Omega_i T_s)}. \tag{4}$$

$$q_0(z) = \frac{(1+z)^{n_0}}{2^{n_0}}, \quad i = 0. \tag{5}$$

Here, $n_0 \in \mathbb{Z}$ is the number of the added zero pairs at the Nyquist frequency. Note that the Q-filter in (3), (4), and (5) is designed assuming an integer N under the sampling time of T_s.